

# Arrays of Plasmonic Nanoparticles Assembled on Patterns of Polymer Brushes Fabricated by Soft Lithography

Hasan H. Ipekci<sup>1,4</sup>  Afia Asif<sup>2,5</sup>  Sema Karabel<sup>3,4</sup>  M. Serdar Onses<sup>3,4</sup> 

<sup>1</sup>Necmettin Erbakan University, Department of Metallurgical and Materials Engineering, Konya, Turkey

<sup>2</sup>Ozyegin University, Department of Electrical and Electronics Engineering, Istanbul, Turkey

<sup>3</sup>Erciyes University, Department of Materials Science and Engineering, Kayseri, Turkey

<sup>4</sup>Erciyes University, Nanotechnology Research Center (ERNAM), Kayseri, Turkey

<sup>5</sup>Technical University of Denmark, Department of Biotechnology and Biomedicine, Kongens Lyngb, Denmark

## ABSTRACT

This work employed end-grafted poly(ethylene glycol) (PEG) and hydroxyl-terminated poly(2-vinylpyridine) (P2VP) polymer chains for selective immobilization and patterning of plasmonic nanoparticles (NPs). A soft lithographic method which called micromolding in capillaries (MIMIC) used in this study. The polymers are deposited the capillary flow by the channels which formed by an elastomeric mold and substrate. The localized coatings are referred as polymer brushes and show great promise in the assembly of NPs due to the tunable interaction between the polymer chains and particles. The results show that the width of patterns defined by the channels is smaller than 1.5  $\mu\text{m}$  with a length of around 0.5 cm. Also, the heights of the patterns are  $\sim 3.5$  nm for P2VP and  $\sim 10$  nm for PEG. The fabricated structures exhibited high levels of plasmonic activity and surface enhanced Raman scattering due to the immobilized Au NPs. The patterning polymer brushes and plasmonic NPs over large areas by a low-cost process show great promise for a variety of applications that range from molecular sensors to biotechnology.

### Keywords:

Soft-lithography, Polymer brushes, Nanoparticles, Plasmonics.

### Article History:

Received: 2020/03/07

Accepted: 2020/09/01

Online: 2020/09/30

Correspondence to: Hasan H. Ipekci,

E-mail: hhipekci@erbakan.edu.tr;

Phone: +90 332 325 20 24 (4000)

## INTRODUCTION

Functionalization of surfaces with polymer brushes shows important promise for a range of applications in materials engineering [1, 2], nanotechnology [3, 4] and biotechnology [5, 6]. A particular area where these end-grafted polymer chains are receiving increasing attention is immobilization and assembly of colloidal NPs [7-9]. The ultra-smooth surfaces, mechanical robustness, long-term durability and ability to tune the chemistry, thickness and grafting density of the brushes present a highly useful platform for benefiting from the interesting properties of NPs that are available in precisely defined size, shape and material composition in massive quantities through wet chemistry approaches [10]. Tailoring the interaction of polymer brushes with NPs through the intrinsic properties such as the length of polymer chains [11] and external stimuli such as pH [12] allows for assembly of particles into specific architectures that can be dynamically tuned. Assembly of NPs into or-

dered structures is particularly critical for plasmonic NPs, since collective properties of these materials arise when they are separated by small gaps [13]. The use of NPs in applications such as sensors [14], structural coloration [15], antennas [16], optoelectronics devices [17] and directing cellular behavior for bioengineering [18], on the other hand, requires methods to control the position of assemblies of particles on the surface of technologically relevant substrates. For these applications, it requires the development of low cost, high efficiency and versatile patterning of polymer brushes for the selective placement and assembly of colloidal NPs.

A variety of different methods exists for fabrication of patterned polymer brushes using methods including electron beam lithography [19], photolithography [20], dip-pen nanolithography [21], and jet printing [22, 23]. These methods have all addressed different aspects such

as high resolution and additive patterning of multiple materials; however, these methods typically suffer from costly and specific setups that are not widely accessible and inability to pattern large areas at short processing times. Self-assembled templates can be used to fabricate polymer brush patterns with periodic features of the certain geometries and dimensions [24, 25]. Soft lithography [26, 27] approaches allow for low-cost, large area patterning of materials using elastomeric stamps usually made from poly(dimethylsiloxane) (PDMS). A commonly adapted approach in patterning polymer brushes is microcontact printing of self-assembled monolayers which serve as initiator molecules for surface-initiated polymerization from sites defined by the stamp [28-32]. Referred as “grafting from”, end-tethered polymer chains grown on the surface have the advantage of achieving high grafting densities and thicknesses. The challenges associated with surface-initiated polymerization include synthesis and characterization of polymers with well-defined molecular weights and polydispersities, lengthy polymerization reactions requiring experienced personnel and specialized tools (e.g. schlenk line) that are not commonly available. A versatile strategy overcoming these challenges is direct attachment of preformed end-functional polymers synthesized and characterized with bulk polymerization techniques. The use of commercially available polymers greatly simplifies the surface functionalization with this approach called as grafting to. The thickness and grafting density of polymer brushes are typically not as high as those that can be achieved with grafting from; however, sufficient for many applications such as nanolithography, engineering of surface wetting, and NP assembly [33-35]. A soft-lithographic approach to patterning preformed end-functional polymers was recently [36] demonstrated using micromolding in capillaries [37] (MIMIC) which is based on capillary flow of fluids through microchannels formed by placing a PDMS mold onto a substrate. Different hydrophilic polymers were synthesized via the reversible addition-fragmentation chain process to include a functional group that can react with a substrate functionalized with self-assembled monolayers presenting diene groups. The resulting patterns were used for surface passivation against biofouling. It remains a challenge to pattern polymer brushes on technologically relevant substrates for organization of plasmonic NPs by one-step grafting of end-functional macromolecules deposited via soft-lithography.

Here we demonstrate fabrication of micropatterns of polymer brushes for selective immobilization and assembly of metallic NPs by MIMIC. The strength of the presented work is that silicon oxide terminated substrates that are widely used in most applications can be patterned with polymer brushes by one-step direct grafting of end-functional polymers. Poly(ethylene glycol) (PEG) and hydroxyl-terminated poly(2-vinylpyridine) (P2VP) were deposited on regions de-

fined by the elastomeric stamp through the capillary flow of the polymer solutions followed by evaporation and removal of the stamp. The polymers were then end-grafted through a fast thermal annealing step to silicon oxide terminated substrates. The localized grafting of P2VP and PEG brushes was studied via optical and atomic force microscopy (AFM). The fabricated patterns served as binding sites for colloidal gold NPs. The functionality and uniformity of the plasmonic NP arrays were demonstrated by mapping their activity in surface-enhanced Raman scattering (SERS).

## MATERIALS AND EXPERIMENTAL PROCEDURES

### Materials

PDMS and curing agent (Sylgard 184) were purchased from Dow Corning. SU-8 2050 was purchased from Microchem Inc. AFM calibration grid (629-30AFM) and Au NPs (20 nm in diameter) were purchased from Ted Pella Inc. Silicon wafers < 100 > were purchased from Wafer World Inc. P2VP-OH (20.5 kg/mol) was purchased from Polymer Source Inc. Methanol, chloroform and *N, N*-dimethylformamide, chlorobenzene were purchased from Merck. PEG (35.0 kg/mol, BioUltra), propylene glycol monomethyl ether acetate (PGMEA), rhodamine 6G and cyclopentanone were purchased from Sigma-Aldrich.

### Fabrication of Master Substrates

SU-8 was diluted with cyclopentanone to achieve films of 10  $\mu\text{m}$  in thickness by spin-coating at 3800 rpm. Patterns of SU-8 were then fabricated by photolithography: pre-bake (95  $^{\circ}\text{C}$  for 4 min.), UV exposure ( $\sim 280$  mJ/cm<sup>2</sup>), post-bake (95  $^{\circ}\text{C}$  for 4 min.), development in PGMEA (5 min). AFM calibration grids were used directly without any processing. The surface of the master substrates was modified with 3-Aminopropyl triethoxysilane before casting PDMS for easy separation of the mold from the substrate following curing.

### Preparation of Elastomeric Molds

The elastomeric molds were prepared by casting the mixture (10:1) of the PDMS and curing agent on top of the master substrates followed by desiccation for 10 min and heating at 65  $^{\circ}\text{C}$  for 2 h. The cured PDMS molds were then separated from the master substrate.

### Patterning of P2VP and PEG brushes Using MIMIC

The elastomeric molds were washed in DMF under sonication for 10 min and then dried at 90  $^{\circ}\text{C}$  for 2 h, prior to the MIMIC process. PDMS molds were then placed on top of the silicon substrates that were freshly cleaned in a UV-ozone chamber (Bioforce, procleaner) for 20 min.

Solutions (~5  $\mu\text{L}$ ) of (1% for AFM grids, 3% for 20  $\mu\text{m}$  wide channels) P2VP-OH in DMF and (1% for AFM grids, 6% for 20  $\mu\text{m}$  wide channels) PEG in methanol were placed near the open-end of the micro-channels. The molds were then removed from the silicon substrate following the filling of the channels and evaporation of the solvents which were monitored under an optical microscope. This process typically took ~2 h. The silicon substrates with the patterns of end-functional polymers were then annealed in a glove-box filled with argon at 180  $^{\circ}\text{C}$  for 5 min for the grafting of chains. The excess and ungrafted polymers were then removed by 3 cycles of sonication in solvents (DMF for P2VP and chloroform for PEG) for 3 min per cycle. The substrates were then dried with nitrogen.

### Selective Immobilization of Plasmonic Nanoparticles on the Patterned Surfaces

Substrates containing patterned substrates were treated with citrate-stabilized Au NPs by spotting a droplet (~100  $\mu\text{L}$ ) of particle solution for 1 h in a humid atmosphere (a petri dish sealed with a parafilm, containing a little water near the substrate). The substrate was then washed in water under sonication for 2 min and dried with nitrogen. A solution of 100  $\mu\text{M}$  rhodamine 6G in ethanol was dropped on the immobilized NPs for investigating the SERS response of the particles.

### Characterization of Patterned Brushes and Nanoparticle Arrays

The process of grafting brushes were investigated by analyzing the topography of patterns following MIMIC, annealing and washing with an AFM (Veeco, Multimode 8). The surface morphology of the master substrates and arrays of NPs were imaged with a SEM (Zeiss EVO LS10) at 20 kV. The activity of the immobilized NPs were investigated via SERS mappings obtained by Witec alpha M+ Raman Microscopy system equipped with a 532 nm laser source, 50x objective (N.A.=0.85), motorized stage at x, y dimensions with 0.1  $\mu\text{m}$  resolution. All Raman spectroscopy measurements were performed with 0.05s acquisition time, 0.1mW laser power, 2  $\mu\text{m}$  spot size diameter. Raman mappings were obtained with 0.5  $\mu\text{m}$  resolution. Each Raman spectra performed baseline correction and Si substrate subtraction.

## RESULTS AND DISCUSSION

The schematic description of the process for fabricating arrays of NPs immobilized on patterns of polymer brushes prepared by MIMIC is presented in Fig. 1. The elastomeric molds were prepared by casting PDMS on top of the master substrates containing linear patterns of trenches using standard soft-lithography procedures. Placing the mold on top of a freshly cleaned silicon sub-

strate resulted in open-ended channels sealed by the conformal contact enabled by the compliant nature of the PDMS. Organic solutions of polymers were spotted near the open end of the channels. We investigated polymers with two different backbone chemistries with identical end-functionality. Hydroxyl-terminated P2VP and PEG were dissolved in DMF and methanol, respectively. The latter polymer has hydroxyl groups at both ends of the polymer. The solutions filled the channels by capillary action and the mold was removed from the substrate following evaporation of the solvent. The resulting patterns of end-functional polymers were then subjected to a brief thermal annealing for grafting of the polymer chains to the substrate. Since the amount of deposited polymer is in excess of grafted chains, ungrafted polymer chains were removed by sonication in DMF and chloroform for P2VP and PEG, respectively. Patterns of polymer brushes then served as templates for guided attachment of colloidal gold nanoparticles which were immobilized by spotting a solution of Au NPs on the entire region followed by washing in water under sonication. After sonication the physically bound NPs removed from the surface. The particles only attached to the patterned polymer brushes, thanks to the well-defined chemical patterning via MIMIC.

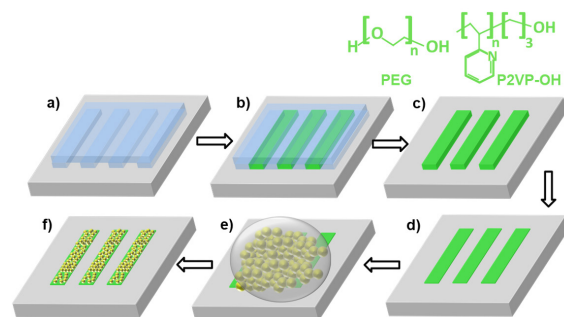


**Figure 1.** Schematic description of the process for fabricating arrays of plasmonic NPs on top of patterns of polymer brushes prepared by a soft-lithography approach. a) An elastomeric mold consisting of PDMS is placed on a silicon substrate forming open-ended channels. b) A drop of end-functional polymers dissolved in an organic solvent is placed at the end of the channels. The polymer solution fills the channel by capillary action. Two polymers are used: hydroxyl-terminated P2VP dissolved in DMF and PEG dissolved in methanol. c) Separation of the mold leads to patterns of end-functional polymers. d) A thermal annealing followed by washing of the excess material leads to grafted polymer chains on the areas defined by the channels. e) A drop of colloidal Au NPs is placed on the entire substrate. f) Au NPs specifically bind to the patterns of polymer brushes.

We employed two different types of master substrates to fabricate the PDMS molds. The master with the large features was fabricated by photolithography using a negative tone photoresist, whereas the other master consisted of a commercially available AFM grid (Fig. 2). The master with the large features consisted of steps with the width of 20  $\mu\text{m}$ , height of 10  $\mu\text{m}$  and period of 100  $\mu\text{m}$ . The grating patterns

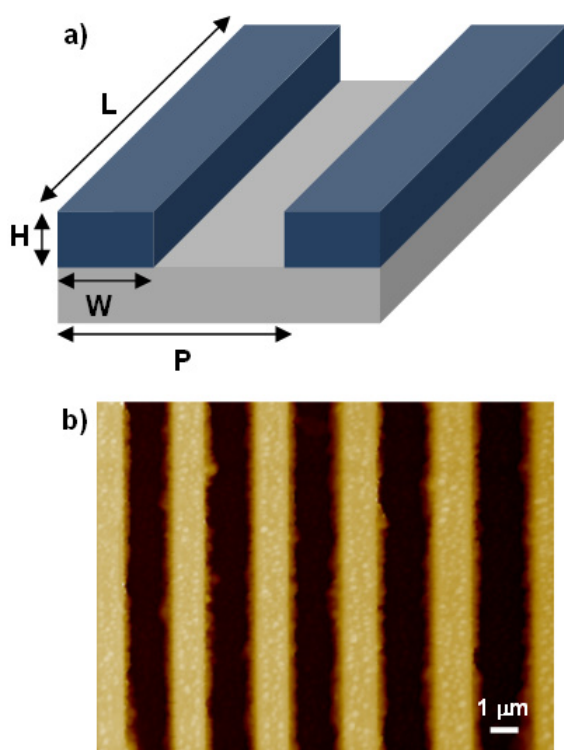


**Figure 2.** Master substrates. a) Schematic description of the dimensions of the master substrates. For the master with the large features:  $L = 5$  mm,  $H = 10$   $\mu\text{m}$ ,  $W = 20$   $\mu\text{m}$ ,  $P = 100$   $\mu\text{m}$ . For the AFM grid:  $L = 2$  mm,  $H = 500$  nm,  $W = 1.5$   $\mu\text{m}$ ,  $P = 3$   $\mu\text{m}$ . b) AFM image of the master substrate consisting of the 1:1 grating patterns.

of the AFM grid had 1:1 ratio of the width to spacing with the width of 1.5  $\mu\text{m}$  and height of  $\sim 500$  nm. The patterns were fabricated with the specified dimension over large areas with the minimum number of defects. Note that the patterns in the mold are complementary to those on the master substrate; however, the patterns on the master are replicated on the surface of the target substrate following MIMIC.

The complete filling of the channels formed by the mold and target substrate by the polymer solutions without loss of the conformal contact is the most critical aspect of patterning polymer brushes with the MIMIC process. Several factors including the surface energy of the channels, surface tension and viscosity of the solutions affect the filling the process [37]. Another important factor for organic solvents, is the swelling of the PDMS molds. Swelling not only can change the dimensions of the patterns, but also can destroy the conformal contact between the PDMS and target substrate. We chose DMF and methanol which swell PDMS at low levels [38], for dissolving P2VP and PEG, respectively. Chlorobenzene used in spin-coating films of PEG, for example, led to immediate loss of the conformal contact of the mold with the substrate. Both polymer solutions completely filled the channels (Fig. 3a,c). The complete filling of the channels with the polymer solutions can be exp-

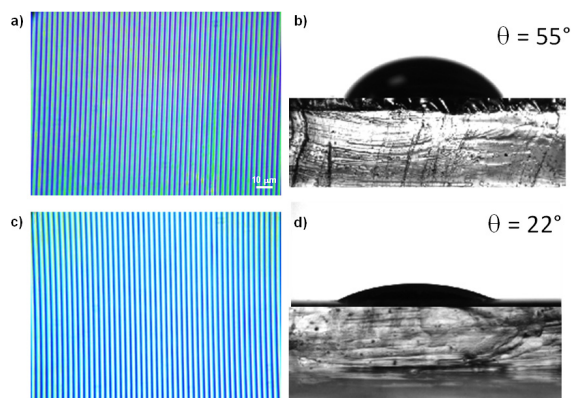


**Figure 3.** Filling of the channels. a, c) Optical microscope images of the target substrates following the MIMIC process and removal of the PDMS mold for a) 1% P2VP-OH in DMF and c) 1% PEG in methanol. b, d) Images of droplets of b) 1% P2VP-OH in DMF and d) 1% PEG in methanol. The contact angle of the droplets are given at the top-right of the image.

lained by their wetting behavior of the silicon substrate and channels (Fig. 3b,d). A solution of (1%) P2VP in DMF had a contact angle of  $55^\circ$  on PDMS and  $<10^\circ$  on silicon wafer. A solution of (1%) PEG in methanol had a contact angle of  $22^\circ$  on PDMS and  $<10^\circ$  on silicon wafer. Since the contact angles of the solutions on both the target and mold substrate is much less than  $90^\circ$ , the filling of the channels are thermodynamically favorable [37]. Note that oxidizing PDMS molds by a plasma treatment can further decrease these contact angles; however, such process leads to the permanent bonding of the PDMS to the bare silicon wafer. The polymer solutions typically filled the channels at a rate of  $\sim 1.1$  mm/s based on the relatively low molecular weight and therefore low viscosity of the solutions.

The height profile of the patterns after MIMIC, annealing and washing steps inform about the localized grafting of brushes. We systematically characterized the height profile of the patterned samples after each step by AFM imaging. The images after each step were taken from the same region of the same substrates for consistency. Fig. 4 presents the results for grafting P2VP and PEG brushes. The average height of the deposited patterns of end-functional polymers was above 200 nm after the MIMIC process. The edges of the patterns were slightly higher for the both polymers. Such edge effects are likely due to transport of materials to the edge regions during the evaporation of the solvent with a phenomena known as the coffee-ring effect [39]. The width of the patterns was  $\sim 1.4$   $\mu\text{m}$  which was defined by the channels (Table 1). The slightly lower width of the patterns in comparison to the width of the channels is probably a result of swelling and distortion of the PDMS molds during the MIMIC process. Thermal annealing of the patterns resulted in a certain level of spreading of the patterns with an increase in the width and decrease in the height of the patterns. Thermal annealing induced flow also led to a parabolic

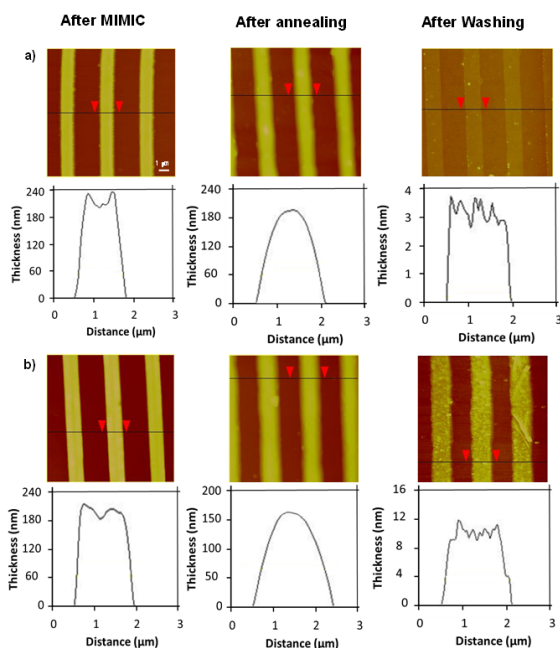


**Figure 4.** Characterization of the height profiles of the patterns following the MIMIC process, grafting and washing steps. a) Grafting of P2VP brushes from 1% P2VP-OH in DMF and b) Grafting of PEG brushes from 1% PEG in methanol.

height profile with the maxima at the center of the pattern. PEG showed a slightly higher extent of spreading than P2VP, which could be related to the lower glass transition of the molecules. The removal of the excess and ungrafted material through washing resulted in grafted polymer chains with heights defined by the molecular weight of the polymers and grafting densities. The height of the patterned polymer brushes was  $\sim 3.5$  nm and  $\sim 10.0$  nm for P2VP and PEG, respectively. These values are slightly lower than the thicknesses ( $\sim 5.3$  nm for P2VP,  $\sim 12.0$  nm for PEG) obtained for brushes grafted in identical conditions from films deposited by spin-coating and correspond to grafting densities of 0.10 and 0.19 for P2VP and PEG brushes, respectively. The final patterns of grafted brushes has a roughness smaller than 1 nm. Irregularities in the center and edges of the patterns following the MIMIC process are not reflected to the patterns of brushes, since only chemically bound polymers remain attached to the substrate following the washing step. The width of the grafted brushes was typically lower than the width of the patterns following the thermal annealing. This interesting observation could be related to the presence of residual PDMS on the silicon in the regions where there was a contact between the mold and substrate. Another factor could be the low heights of the patterns in the edge regions following the thermal annealing step.

Arrays of plasmonic NPs over large areas can be readily achieved on patterns of P2VP and PEG brushes prepared by the MIMIC process. Patterned P2VP and PEG brushes surrounded by silicon oxide serve as binding sites for the

**Table 1.** The width and height of the patterns after different steps.

Brush	Step	Width ( $\mu$ m)	Height (nm)
P2VP	After Mimic	$1.33 \pm 0.03$	$237.92 \pm 11.48$
	After Annealing	$1.68 \pm 0.03$	$215.31 \pm 9.15$
	After Washing	$1.42 \pm 0.04$	$3.50 \pm 0.27$
PEG	After Mimic	$1.43 \pm 0.03$	$218.67 \pm 9.50$
	After Annealing	$1.94 \pm 0.03$	$189.67 \pm 6.80$
	After Washing	$1.70 \pm 0.13$	$10.0 \pm 0.65$

selective immobilization of citrate-stabilized Au NPs. SEM images presented in Fig. 5 show that colloidal Au NPs attached to the patterns with a high level of specificity, i.e. the particles bound at high densities on the patterns with none or negligible binding to the background regions. The high level of specificity is a consequence of several factors: i) The MIMIC process enables additive patterning of materials without deposition of the materials to the background regions, thanks to the compliant nature of PDMS. ii) Citrate-stabilized Au NPs have a strong binding affinity towards P2VP and PEG brushes, allowing strong washing of the substrates under sonication following the immobilization of the particles. iii) The absence of interaction between the citrate-stabilized Au NPs and silicon oxide terminated background regions results in low levels of immobilized particles which are removed in the washing step. SEM images show that uniform arrays of particles could be obtained in widths defined by the mold. The use of molds with widths as small as several hundred nanometers could be possible based on the previously reported soft-lithography studies; however, several factors[40] such as incomplete filling and distortion in the patterns prevent from scaling down this process below 100 nm. We found that the number of immobilized Au NPs was significantly higher on the patterned PEG brushes in comparison to homogenous PEG brushes deposited by spin-coating. The number of immobilized Au NPs (20 nm in diameter) per square micrometer was  $778 \pm 11$  and this number reduced to  $246 \pm 8$  particles on homogenous PEG brushes. This result is consistent with the previous study [11] where the density of bound particles on lithographically patterned PEG brushes was higher in comparison to homogenous substrates. It is likely that the kinetics of particle adsorption is enhanced by generating PEG brush grafted patterns surrounded by regions where there is no interaction with the Au NPs. The density of immobilized particles on patterned P2VP brushes, on the other hand, was  $287 \pm 7$  NPs/ $\mu$ m<sup>2</sup> which is consistent with the values observed on homogenous PEG brushes deposited by spin-coating [41]. The contrast in the variance of the density of immobilized NPs between the patterned and homogeneous substrates for PEG and P2VP brushes probably relates to the different types of polymer-particle interaction.

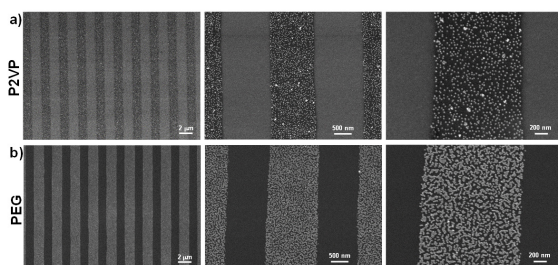


**Figure 5.** SEM images of the NP arrays. a) P2VP and b) PEG brushes. The diameter of the particles is 20 nm.

We finally investigated the functionality, uniformity and reproducibility of the patterned gold nanoparticles by mapping the SERS response of the fabricated substrates. Localized surface plasmon resonances of metallic nanostructures result in electromagnetic enhancement of signals observed in Raman spectroscopy [42]. Therefore, mapping the characteristic peak of a reporter molecule in Raman spectroscopy directly informs about the functionality and uniformity of the fabricated NP arrays. Fig. 6 and Fig. 7 summarizes SERS results on the arrays of NPs generated on patterns of P2VP and PEG brushes using rhodamine 6G as the reporter molecule. The peaks positioned at 611, 774, 1184, 1311, 1361, 1507, 1573 and 1648  $\text{cm}^{-1}$  were detected on the immobilized NPs. The mapping of the peak at a position of 1361  $\text{cm}^{-1}$  shows specific and strong signals are received from the patterns where Au NPs are located. An interesting result is that the intensity of signals was higher for NPs immobilized on the patterned brushes in comparison to homogenous brushes prepared by spin-coating (Fig. 6.c). Two factors contribute to such enhancement of the signals. First, the density of particles per unit area is larger in the case of patterned brushes, resulting in higher density of scattering centers. Second, the placement of NPs in close-proximity results in areas where electromagnetic fields are focused in small gaps called as hot-spots. The mapping of the SERS response also inform about the uniformity of the density of the bound particles over areas that are much larger than that can be observed by SEM imaging. The intensity of the signals from the patterns was mostly uniform; however, some of the lines had regions of weak SERS response. We found out that the density of particles in these defective regions are lower than the rest of the patterns. These defective regions were typically less than 10% of the total area and probably formed as a result of issues during the MIMIC process such as contaminations from the PDMS molds. To show the reproducibility of the patterned gold nanoparticles, SERS spectrum was measured at 50 randomly selected regions. (Fig. 7a,b). The SERS spectrum was measured at 15 randomly selected regions and showed that a relatively uniform and RSD value of the RG6 at 1361  $\text{cm}^{-1}$  was 6.7% and 5.9% for the PEG and P2VP, respectively (Fig. 7c,d).

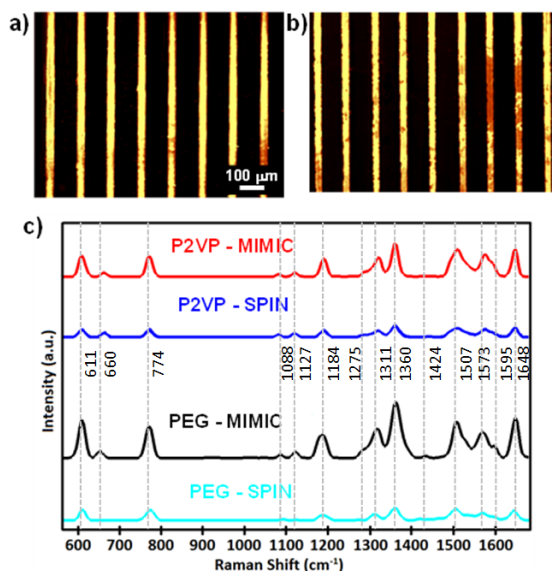


**Figure 6.** SERS results on the patterned P2VP and PEG brushes. Raman mapping of rhodamine 6G on patterns of a) P2VP and b) PEG brushes. c) Raman scattering spectra of rhodamine 6G on immobilized particles. The diameter of the particles is 60 nm.

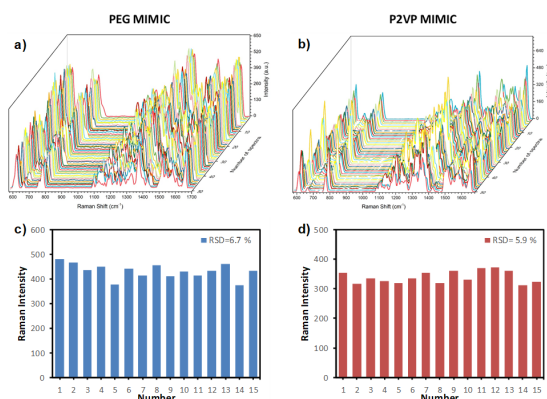


**Figure 7.** SERS spectra of rhodamine were collected from 50 random points on patterns of a) PEG and b) P2VP brushes. Relative standard deviation (RSD) of specific Raman modes at 1361  $\text{cm}^{-1}$  of the 15 random points c) PEG and d) P2VP brushes.

## CONCLUSION

A soft lithographic approach relying on capillary flow of solutions containing end-functional P2VP and PEG molecules into channels is used to fabricate patterns of polymer brushes. This approach enables low-cost, large area patterning of end-grafted polymer chains via one-step grafting reaction. The lateral dimensions of the patterns are defined by the mold, whereas the height of the resulting brushes are determined by the grafting process as a function of the chain length and grafting length. The ability to pattern end-grafted polymer chains with a high level of specificity allowed for fabrication of pat-

terned assemblies of plasmonic NPs which show strong SERS effects. This platform can serve as foundation for advanced sensor systems through integration of multiple analyte molecules on the plasmonic NPs using microfluidic channels. The backbone chemistry of the patterned polymers as well as colloidal NPs can be varied according to the needs of specific applications.

## ACKNOWLEDGEMENT

This work was supported by Scientific and Technological Research Council of Turkey (TUBITAK) Grant No. 115M220.

## References

- Sugnaux C, Mallorqui AD, Herriman J, Klok HA, Morral, AFI. Polymer Brush Guided Formation of Conformal, Plasmonic Nanoparticle-Based Electrodes for Microwire Solar Cells. *Adv Funct Mater* 25 (2015) 3958–3965.
- Ipekci HH, Arkaz HH, Onses MS, Hancer, M. Superhydrophobic coatings with improved mechanical robustness based on polymer brushes. *Surf Coat Tech* 299 (2016) 162–168.
- Mansky P, Liu Y, Huang E, Russell TP, Hawker, CJ. Controlling polymer–surface interactions with random copolymer brushes. *Science* 275 (1997) 1458–1460.
- Thode CJ, Cook PL, Jiang YM, Onses MS, Ji SX, Himpfel FJ, Nealey, PF. In situ metallization of patterned polymer brushes created by molecular transfer print and fill. *Nanotechnology* 24 (2013).
- Kroning A, Furchner A, Aulich D, Bittrich E, Rauch S, Uhlmann P, Eichhorn KJ, Seeber M, Luzinov I, Kilbey SM, Lokitz BS, Minko S, Hinrichs, K. In Situ Infrared Ellipsometry for Protein Adsorption Studies on Ultrathin Smart Polymer Brushes in Aqueous Environment. *ACS Appl Mater Inter* 7 (2015) 12430–12439.
- Yu K, Lo JCY, Mei Y, Haney EF, Siren E, Kalathottukaren MT, Hancock REW, Lange D, Kizhakkedathu, JN. Toward Infection-Resistant Surfaces: Achieving High Antimicrobial Peptide Potency by Modulating the Functionality of Polymer Brush and Peptide. *ACS Appl Mater Inter* 7 (2015) 28591–28605.
- Onses MS, Liu CC, Thode CJ, Nealey, PF. Highly Selective Immobilization of Au Nanoparticles onto Isolated and Dense Nanopatterns of Poly(2-vinyl pyridine) Brushes down to Single-Particle Resolution. *Langmuir* 28 (2012) 7299–7307.
- Nguyen M, Kanaev A, Sun XN, Lacaze E, Lau-Truong S, Lamouri A, Aubard J, Felidj N, Mangeney, C. Tunable Electromagnetic Coupling in Plasmonic Nanostructures Mediated by Thermoresponsive Polymer Brushes. *Langmuir* 31 (2015) 12830–12837.
- Christau S, Genzer J, Klitzing, RV. Polymer Brush/Metal Nanoparticle Hybrids for Optical Sensor Applications: from Self-Assembly to Tailored Functions and Nanoengineering. *Zeitschrift Fur Physikalische Chemie-International Journal of Research in Physical Chemistry & Chemical Physics* 229 (2015) 1089–1117.
- Lu XM, Rycenga M, Skrabalak SE, Wiley B, Xia, YN. Chemical Synthesis of Novel Plasmonic Nanoparticles. *Annu Rev Phys Chem* 60 (2009) 167–192.
- Onses MS, Nealey, PF. Tunable Assembly of Gold Nanoparticles on Nanopatterned Poly(ethylene glycol) Brushes. *Small* 9 (2013) 4168–4174.
- Tokareva I, Minko S, Fendler JH, Hutter, E. Nanosensors based on responsive polymer brushes and gold nanoparticle enhanced transmission surface plasmon resonance spectroscopy. *J Am Chem Soc* 126 (2004) 15950–15951.
- Romo-Herrera JM, Alvarez-Puebla RA, Liz-Marzan, LM. Controlled assembly of plasmonic colloidal nanoparticle clusters. *Nanoscale* 3 (2011) 1304–1315.
- Liu Y, Xie SW, Xiao X, Li SH, Gao FH, Zhang ZY, Du, JL. Fabricating metal nanoparticle arrays at specified and localized regions of microfluidic chip for LSPR sensing. *Microelectron Eng* 151 (2016) 7–11.
- Wang GP, Chen XC, Liu S, Wong CP, Chu, S. Mechanical Chameleon through Dynamic Real Time-Plasmonic Tuning. *ACS Nano* 10 (2016) 1788–1794.
- Liu N, Tang ML, Hentschel M, Giessen H, Alivisatos, AP. Nanoantenna-enhanced gas sensing in a single tailored nanofocus. *Nat Mater* 10 (2011) 631–636.
- Kim BH, Onses MS, Lim JB, Nam S, Oh N, Kim H, Yu KJ, Lee JW, Kim JH, Kang SK, Lee CH, Lee J, Shin JH, Kim NH, Leal C, Shim M, Rogers, JA. High-Resolution Patterns of Quantum Dots Formed by Electrohydrodynamic Jet Printing for Light-Emitting Diodes. *Nano Lett* 15 (2015) 969–973.
- Zhu M, Baffou G, Meyerbroeker N, Polleux, J. Micropatterning Thermoplasmonic Gold Nanoarrays To Manipulate Cell Adhesion. *ACS Nano* 6 (2012) 7227–7233.
- Kim SO, Solak HH, Stoykovich MP, Ferrier NJ, Pablo JJ, Nealey, PF. Epitaxial self-assembly of block copolymers on lithographically defined nanopatterned substrates. *Nature* 424 (2003) 411–414.
- Poelma JE, Fors BP, Meyers GF, Kramer JW, Hawker, CJ. Fabrication of Complex Three-Dimensional Polymer Brush Nanostructures through Light-Mediated Living Radical Polymerization. *Angew Chem Int Edit* 52 (2013) 6844–6848.
- Chen CJ, Zhou XC, Xie Z, Gao TT, Zheng, ZJ. Construction of 3D Polymer Brushes by Dip-Pen Nanodisplacement Lithography: Understanding the Molecular Displacement for Ultrafine and High-Speed Patterning. *Small* 11 (2015) 613–621.
- Onses MS, Ramirez-Hernandez A, Hur SM, Sutanto E, Williamson L, Alleyne AG, Nealey PF, Pablo JJ, Rogers, JA. Block Copolymer Assembly on Nanoscale Patterns of Polymer Brushes Formed by Electrohydrodynamic Jet Printing. *ACS Nano* 8 (2014) 6606–6613.
- Parry AV, Straub AJ, Villar-Alvarez EM, Phuengphol T, Nicoli JE, Lim X, WK, Jordan LM, Moore KL, Taboada P, Yeates, SG. Sub-Micron Patterning of Polymer Brushes: An Unexpected Discovery from Inkjet Printing of Polyelectrolyte Macroinitiators. *J Am Chem Soc* (2016).
- Onses MS. Fabrication of Nanopatterned Poly(ethylene glycol) Brushes by Molecular Transfer Printing from Poly(styrene-block-methyl methacrylate) Films to Generate Arrays of Au Nanoparticles. *Langmuir*. 31 (2015) 1225–1230.
- Li YF, Zhang JH, Fang LP, Jiang LM, Liu WD, Wang TQ, Cui LY, Sun HC, Yang, B. Polymer brush nanopatterns with

- controllable features for protein pattern applications. *J Mater Chem* 22 (2012) 25116–25122.
26. Weibel DB, DiLuzio WR, Whitesides, GM. Microfabrication meets microbiology. *Nat Rev Microbiol* 5 (2007) 209–218.
  27. Singh A, Kulkarni SK, Khan–Malek, C. Patterning of SiO<sub>2</sub> nanoparticle–PMMA polymer composite microstructures based on soft lithographic techniques. *Microelectron Eng* 88 (2011) 939–944.
  28. Zhou F, Zheng ZJ, Yu B, Liu WM, Huck, WTS. Multicomponent polymer brushes. *J Am Chem Soc* 128 (2006) 16253–16258.
  29. Chen T, Jordan R, Zauscher, S. Dynamic Microcontact Printing for Patterning Polymer–Brush Microstructures. *Small* 7 (2011) 2148–2152.
  30. Rolling O, De Bruycker K, Vonhoren B, Stricker L, Korsgen M, Arlinghaus HF, Ravoo BJ, Du Prez, FE. Rewritable Polymer Brush Micropatterns Grafted by Triazolinedione Click Chemistry. *Angew Chem Int Edit* 54 (2015) 13126–13129.
  31. Diamanti S, Arifuzzaman S, Elsen A, Genzer J, Vaia, RA. Reactive patterning via post–functionalization of polymer brushes utilizing disuccinimidyl carbonate activation to couple primary amines. *Polymer* 49 (2008) 3770–3779.
  32. Chen T, Jordan R, Zauscher, S. Extending micro–contact printing for patterning complex polymer brush microstructures. *Polymer* 52 (2011) 2461–2467.
  33. Felts JR, Onses MS, Rogers JA, King, WP. Nanometer Scale Alignment of Block–Copolymer Domains by Means of a Scanning Probe Tip. *Adv Mater* 26 (2014) 2999–3002.
  34. Liu XY, Biswas S, Jarrett JW, Poutrina E, Urbas A, Knappenberger KL, Vaia RA, Nealey, PF. Deterministic Construction of Plasmonic Heterostructures in Well–Organized Arrays for Nanophotonic Materials. *Adv Mater* 27 (2015) 7314–+.
  35. Onses MS, Wan L, Liu XY, Kiremitler NB, Yilmaz H, Nealey, PF. Self–Assembled Nanoparticle Arrays on Chemical Nanopatterns Prepared Using Block Copolymer Lithography. *ACS Macro Lett* 4 (2015) 1356–1361.
  36. Vonhoren B, Langer M, Abt D, Barner–Kowollik C, Ravoo, BJ. Fast and Simple Preparation of Patterned Surfaces with Hydrophilic Polymer Brushes by Micromolding in Capillaries. *Langmuir* 31 (2015) 13625–13631.
  37. Kim E, Xia YN, Whitesides, GM. Micromolding in capillaries: Applications in materials science. *J Am Chem Soc* 118 (1996) 5722–5731.
  38. Lee JN, Park C, Whitesides, GM. Solvent compatibility of poly(dimethylsiloxane)–based microfluidic devices. *Anal Chem* 75 (2003) 6544–6554.
  39. Yunker PJ, Still T, Lohr MA, Yodh, AG. Suppression of the coffee–ring effect by shape–dependent capillary interactions. *Nature* 476 (2011) 308–311.
  40. Xia YN, Whitesides, GM. Soft lithography. *Angew Chem Int Edit* 37 (1998) 550–575.
  41. Yilmaz H, Pekdemir S, Ipekci HH, Kiremitler NB, Hancer M, Onses, MS. Ambient, rapid and facile deposition of polymer brushes for immobilization of plasmonic nanoparticles. *Appl Surf Sci* 385 (2016) 299–307.
  42. Shalabaeva V, La Rocca R, Miele E, Dipalo M, Messina GC, Perrone M, Maidecchi G, Gentile F, De Angelis, F. Plasmonic microholes for SERS study of biomolecules in liquid. *Microelectron Eng* 158 (2016) 59–63.